16 Feb 2023

Synthesis of Enantiomers of Chiral Ester Derivatives Containing an Amide Group and their Chiral Recognition by ^{1}H NMR Spectroscopy

Yan Lin Li

Hong Mei Zhao

Yu Qing Ren

Meng Qiu

et. al. For a complete list of authors, see https://scholarsmine.mst.edu/chem_facwork/3214

Recommended Citation

Y. L. Li et al., "Synthesis of Enantiomers of Chiral Ester Derivatives Containing an Amide Group and their Chiral Recognition by ^{1}H NMR Spectroscopy," *ChemistrySelect*, vol. 8, no. 7, article no. e202204039, Wiley, Feb 2023.

The definitive version is available at https://doi.org/10.1002/slct.202204039

Chemistry Europe
European Chemical Societies Publishing

WILEY VCH

Excellence in Chemistry Research

Announcing our new flagship journal

- Gold Open Access
- Publishing charges waived
- Preprints welcome
- Edited by active scientists

Meet the Editors of *ChemistryEurope*

Luisa De Cola
Università degli Studi di Milano Statale, Italy

Ive Hermans
University of Wisconsin-Madison, USA

Ken Tanaka
Tokyo Institute of Technology, Japan

ChemistrySelect

Research Article
doi.org/10.1002/slct.202204039

Chemistry Europe
European Chemical Societies Publishing

www.chemistryselect.org

Synthesis of Enantiomers of Chiral Ester Derivatives Containing an Amide Group and Their Chiral Recognition by ^{1}H NMR Spectroscopy

Yan-Lin Li,[a] Hong-Mei Zhao,[b] Yu-Qing Ren,[a] Meng Qiu,[a] Hai-Tong Zhang,[a] Guang-Peng Gao,[a] Li Zheng,[a] Pericles Stavropoulos,[c] and Lin Ai*[a]

Enantiomers of chiral ester derivatives containing an amide group, and possessing one or two stereogenic centers were prepared from *L*- and *D*-α-amino acids, and glycine with (*S*)- and (*R*)-mandelic acid for probing their chiral recognition as a new class of chiral guests by ^{1}H NMR spectroscopy, since chiral ester derivatives have been rarely used as chiral substrates for chiral recognition by ^{1}H NMR technology. The results indicated that these chiral ester derivatives have been successfully differentiated in the presence of tetraaza macrocyclic chiral solvating agents (TAMCSAs) **1a**–**1c**. In order to better understand their chiral discriminating behavior, Job plots, association constants (K_a), and theoretical calculations of (*S*,*S*)-G**1** and (*R*,*R*)-G**1**, as a representative example, were performed, respectively. In order to evaluate their practical application, the ^{1}H NMR spectra of G**1** and G**9** with various optical purities were measured (up to 98% ee). In this work, a practical strategy has been effectively established for chiral recognition of chiral ester derivatives containing an amide group and possessing one or two chiral centers in the presence of tetraaza macrocyclic chiral solvating agents **1a**–**1c** by means of ^{1}H NMR spectroscopy.

Introduction

Chiral phenomena are ubiquitous in nature, and play an extremely vital role in the field of various scientific endeavors and practical applications, including in biological systems, asymmetric catalysis and chiral materials.[1] Especially in pharmacology and clinical medicine, two enantiomers of a chiral drug may have dramatically different biological activities and pharmacological effects (even toxic ones).[2] Therefore, it is essential to focus on the development of variously effective methods and techniques for determination of absolute configuration and analysis of optical purity of a chiral drug. Nowadays, most effective methods or strategies for these purposes are mainly relying on chromatography, including gas chromatography (GC)[3] and high-performance liquid chromatography (HPLC),[4] as well as spectroscopy, such as circular dichroism (CD),[5] electronic and vibrational circular dichroism (ECD and VCD),[6] UV-vis and fluorescence[7] and nuclear magnetic resonance (NMR).[8] Among them, chiral HPLC equipped with all kinds of chiral stationary phases has been widely used for the separation of enantiomers and determination of enantiomeric excess of chiral compounds.[9] However, this technique is generally time-consuming, requires expensive organic solvents, often needs special equipment and even complicated sample pretreatment.[10] If there were a faster, simpler and more efficient way for this purpose, it would greatly promote the rapid evaluation of enantiomeric excess in fundamental research and practical applications. To address some of these challenges, the NMR technique has recently attracted more attention, owing to its several obvious advantages, such as simple and convenient operation, accurate and reliable measurement, and employment of low amounts of samples and solvents, facilitated by the ubiquitous availability of NMR spectrometers in nearly all chemical laboratories.[11] Thus, a highly effective, sensitive and versatile chiral solvating agent has become the most vital factor in the process. For this purpose, a variety of chiral solvating agents with different structural features has been designed, synthesized and screened, to further promote rapid development of chiral recognition by ^{1}H NMR spectroscopy.[12] In this paper, tetraaza macrocyclic chiral solvating agents (TAMCSAs) **1a**–**1c** have been synthesized for probing chiral recognition of chiral ester derivatives containing an amide moiety and possessing one or two stereogenic centers by means of ^{1}H NMR spectroscopy (Figure 1).

Results and Discussion

Chiral dicarbamates **3** (R=Ph, Me and Bn) were prepared and cleaved to obtain chiral diamines **4** based on the reported procedure.[13] Chiral diimines **5** were derived from **4** with 3,5-dibromo-2-hydroxybenzaldehyde in dried CH_3OH under reflux.[14] TAMCSAs **1a**–**1c** were synthesized by the intra-

[a] *Y.-L. Li, Y.-Q. Ren, M. Qiu, H.-T. Zhang, G.-P. Gao, L. Zheng, Prof. Dr. L. Ai*
College of Chemistry
Beijing Normal University
Beijing 100875, P. R. China
E-mail: linai@bnu.edu.cn
[b] *Prof. Dr. H.-M. Zhao*
State Key Laboratory of Information Photonics and Communications, School of Science
Beijing University of Posts and Telecommunications
Beijing 100876, P. R. China
[c] *Prof. Dr. P. Stavropoulos*
Department of Chemistry
Missouri University of Science and Technology
Rolla, Missouri 65409, USA

Supporting information for this article is available on the WWW under https://doi.org/10.1002/slct.202204039

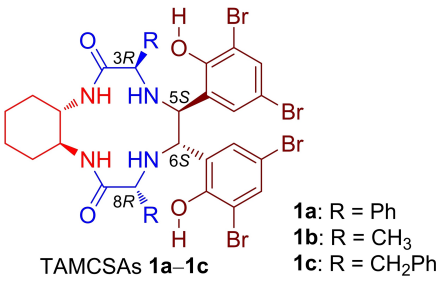

Figure 1. The structures of TAMCSAs **1a–1c**.

molecular reductive C–C coupling reaction of **5** under nitrogen atmosphere in a suspension of activated Zn powder and MsOH from −18 °C to room temperature in 14–20% isolated yields.[15] Other isomers were not found in the cyclization reaction. Additionally, chiral compounds **2a–2c** were obtained as co-products in 15–20% isolated yields (Scheme 1).

The structures of TAMCSAs **1a–1c**, chiral compounds **2a–2c** and **5a–5c** were characterized as new compounds by ^{1}H NMR and ^{13}C NMR spectroscopy together with high-resolution mass spectroscopy (HRMS). NOESY spectra were measured for the correct assignment of absolute configurations of the newly generated chiral carbon atoms of TAMCSAs **1a–1c**. Their NOESY spectra show that the two α-H (R*CH*) protons (*D*-amino acid moieties) of TAMCSAs **1a–1c** show strong NOESY correlated ^{1}H NMR signals with the two newly generated chiral

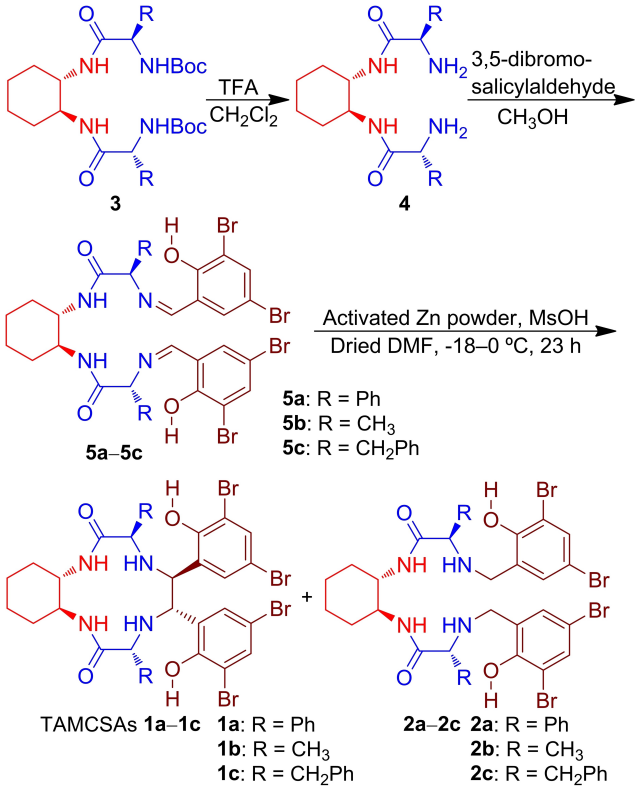

Scheme 1. Synthesis of TAMCSAs **1a–1c**.

carbon atoms (Ar*CH**NH groups). This result suggests that two pairs of protons (α-*H* and Ar*CH**NH) of TAMCSAs **1a–1c** in close proximity are located on the same side of the macrocyclic framework. The results indicated that these two newly generated chiral carbon atoms (carbon-5 and carbon-6) possess *S* and *S* absolute configurations, based on these related ^{1}H NMR signal correlation with respect to the known absolute configuration (*R*) of α-H (amino acid unit) of TAMCSAs **1a–1c** (Figure 1). NOESY spectra of TAMCSAs **1a–1c** are available in the SI.

Herein, key structural features of TAMCSAs **1a–1c** include several polar functional groups (CONH, NH and OH) as potential hydrogen bonding sites, as well as a C_2-symmetric axis and a 12-membered cavity, to facilitate the formation of intermolecular hydrogen bonding with chiral substrates. In addition, the heavy bromine atoms were introduced into the molecular structure of TAMCSAs **1a–1c** for enhancing steric hindrance and electronic effects, to promote their chiral discriminating capability.[16]

Enantiomers (*S*,*S*)- and (*R*,*R*)-G**1**-**11** of chiral ester derivatives with two chiral centers were prepared by the amidation reaction between (*R*)- or (*S*)-mandelic acid and the corresponding *D*- or *L*-amino acid methyl esters, respectively.[17] In addition, enantiomers (*S*)- and (*R*)-G**12** of the chiral ester derivative with only one chiral center, were also prepared from (*S*)- or (*R*)-mandelic acid with methyl 2-aminoacetate according to the same synthetic procedure (Scheme 2).

All new compounds were characterized by ^{1}H NMR and ^{13}C NMR spectroscopy, HRMS and IR methods with the exception of (*S*,*S*)-G**2**–G**4**, (*S*,*S*)-G**9**–G**11** and (*R*)-G**12** as known compounds.

Subsequently, in order to evaluate the chiral discriminating capability of TAMCSAs **1a–1c** towards these chiral ester derivatives, a solution of (±)-G**1** with TAMCSA **1a** with 1:1 molar ratio was prepared at a concentration of 10 mM in $CDCl_3$ (0.5 mL) and its ^{1}H NMR spectrum was measured on a 400 MHz NMR spectrometer. The ^{1}H NMR signals of three types of protons (Ph*CH*NH, Ph*CH*OH and O*CH*$_3$ groups) of (±)-G**1** were split in the presence of TAMCSA **1a**, respectively. Compared with the chemical shift values (δ, ppm) of the corresponding protons of free (±)-G**1** (Figure 2(a)), the δ values of the protons of Ph*CH*NH group of (*S*,*S*)-G**1** (●), and Ph*CH*OH group of (*S*,*S*)-G**1** (●) and (*R*,*R*)-G**1** (○), exhibited downfield shifts. On the contrary, the δ values of the protons of Ph*CH*NH group of (*R*,*R*)-G**1** (○), and O*CH*$_3$ group of (*S*,*S*)-G**1** (●) and (*R*,*R*)-G**1** (○) exhibited upfield shifts (Figure 2(b)). The nonequivalent chemical shift values (ΔΔδ, ppm) of the protons of Ph*CH*NH, Ph*CH*OH and O*CH*$_3$ groups of (±)-G**1** were found to be 0.045, 0.083 and 0.031 ppm, respectively. Subsequently, a sample of (*S*,*S*)-G**1** was added to the aforementioned solution, and its ^{1}H NMR spectrum was measured on a 400 MHz NMR spectrometer. The assignment of absolute configuration of enantiomers of (±)-G**1** was correctly determined based on the change of integration of the ^{1}H NMR signals of the related protons of (±)-G**1** (Figure 2).

In order to obtain better chiral discriminating conditions, first, samples of (±)-G**1** with TAMCSA **1a** (molar ratio = 1:1)

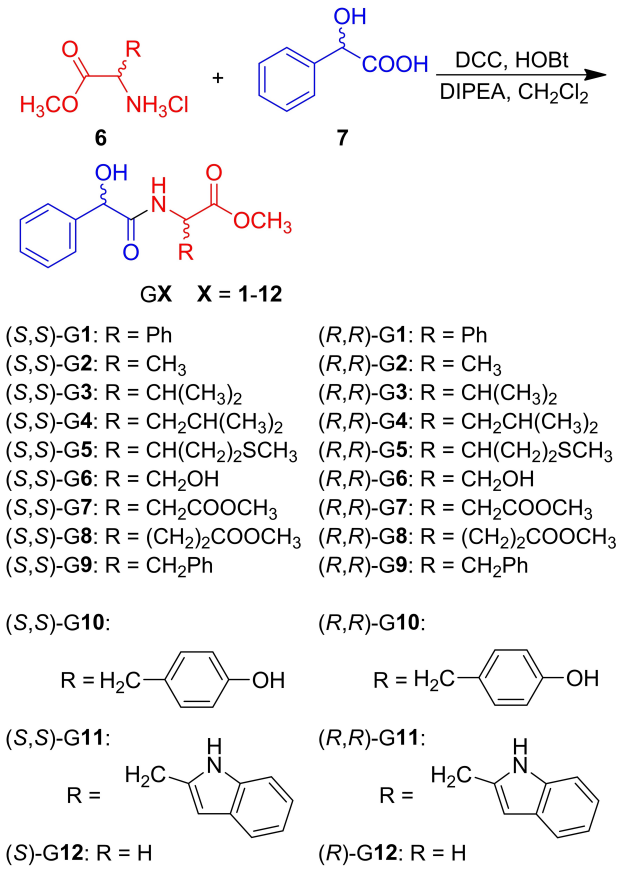

Scheme 2. Synthesis of enantiomers of chiral ester derivatives (±)-G**1**–**12**.

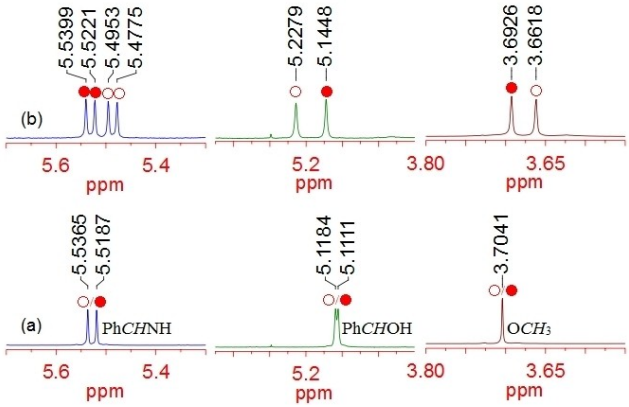

Figure 2. Partial spectra of free (±)-G**1** (a), and (±)-G**1** in the presence of TAMCSA **1 a** (b). "●" and "○" stand for (*S*,*S*)-G**1** and (*R*,*R*)-G**1**, respectively. (±)-G**1**:TAMCSA **1 a** = 1 : 1 (molar ratio), [(±)-G**1**] = 10 mM.

were prepared in different deuterared solvents, such as $CDCl_3$, $CDCl_3$ containing 10% benzene-d_6, acetone-d_6, methanol-d_4 and DMSO-d_6, at a concentration of 10 mM, and their ^{1}H NMR spectra were measured on a 400 MHz spectrometer. The results were summarized in Table 1.

As shown in Table 1, compared with ΔΔδ values of protons of PhC*H*NH (0.045 ppm), PhC*H*OH (0.083 ppm), and OCH_3 (0.031 ppm) groups of (±)-G**1** in $CDCl_3$, ΔΔδ values of the corresponding protons were found to be 0.041, 0.080 and 0.028 ppm (10% benzene-d_6) and 0.018, 0.030 and 0.010 ppm (10% acetone-d_6), respectively. Upon increasing solvent polarity, the separated ^{1}H NMR signals of the corresponding protons of (±)-G**1** cannot be observed in methanol-d_4 and DMSO-d_6 in the presence of TAMCSA **1 a**. Based on these results, $CDCl_3$ is more suitable for chiral recognition in this work.

Table 1. Nonequivalent chemical shift values (ΔΔδ, ppm) of the split proton signals of (±)-G**1** in the presence of TAMCSA **1 a** in different deuterared solvents (400 MHz).[a]

Solvents	PhC*H*NH	PhC*H*OH	OCH_3
$CDCl_3$	0.045	0.083	0.031
$CDCl_3/C_6D_6$ (10%)	0.041	0.080	0.028
$CDCl_3/CD_3COCD_3$ (10%)	0.018	0.030	0.010
$CDCl_3/CD_3OD$ (10%)	0	0	0
$CDCl_3/CD_3SOCD_3$ (10%)	0	0	0

[a] (±)-G**1**: TAMCSA **1 a** = 1 : 1 (molar ratio), [(±)-G**1**] = 10 mM.

Subsequently, to assess the effect of concentration, samples of (±)-G**1** with various concentrations (2.0, 5.0, 7.5, 10.0 and 12.5 mM) were prepared in the presence of TAMCSA **1 a** (molar ratio = 1 : 1) in $CDCl_3$, and their ^{1}H NMR spectra were measured on a 400 MHz spectrometer. The overlaid ^{1}H NMR spectra exhibited gradually increasing ΔΔδ values of the PhC*H*NH proton of (±)-G**1** with increasing concentration (see SI, Figure S1). Based on the solubility of TAMCSA **1 a** and (±)-G**1**, and suitable nonequivalent chemical shift values, a concentration of 10 mM was adopted in this work.

Finally, samples of (±)-G**1** and TAMCSA **1 a** with various molar ratios from 5 : 2 to 2 : 5 were prepared according to their solubility in $CDCl_3$, and their ^{1}H NMR spectra were measured on a 400 MHz spectrometer. The results suggest that the ΔΔδ values of the *CH* proton (PhC*H*OH) of (±)-G**1** are gradually increasing as molar ratios of (±)-G**1** with TAMCSA **1 a** are varied from 5 : 2 to 2 : 5 (see SI, Figure S2). Based on convenient ΔΔδ values, better baseline resolution, and the solubility of TAMCSAs **1 a** and (±)-G**1**, a 1 : 1 molar ratio of (±)-G**1** with TAMCSA **1 a** was used in this study.

To further investigate the discrimination of enantiomers of other chiral ester derivatives, under the optimized chiral discriminating conditions, a series of samples of (±)-G**1**–**12** with TAMCSAs **1 a**–**1 c** (molar ratio = 1 : 1) were prepared in $CDCl_3$, with the exception of (±)-G**1** with TAMCSA **1 a**, and their ^{1}H NMR spectra were recorded on a 400 MHz spectrometer. The results indicate that all enantiomers of (±)-G**1**–**12** were differentiated based on the separated ^{1}H NMR signals of related protons, with the exception of (±)-G**6** in the presence of TAMCSA **1 c**. Subsequently, the assignments of absolute configuration of (±)-G**1**–**12** were determined by adding (*S*,*S*)-G**1**–**11** and (*S*)-G**12** to the corresponding samples noted above. The ΔΔδ values for the split protons of (±)-G**1**–**12** were calculated and summarized in Table 2. The ^{1}H NMR spectra of (±)-G**1**–**12** in the presence of TAMCSAs **1 a**–**1 c** are available in the SI.

Table 2. Nonequivalent chemical shift values (ΔΔδ, ppm) of the split protons of (±)-G**1**–**12** in the presence of TAMCSAs **1 a**–**1 c** in $CDCl_3$ (400 MHz).[a]

Guest/TAMCSA	proton	ΔΔδ	Guest/TAMCSA	proton	ΔΔδ
(±)-G**1**/**1 a**	O*CH*$_3$	0.031	(±)-G**5**/**1 c**	O*CH*$_3$	0.012
	*CH*OH	0.083		*CH*OH	0.021
	*CH*NH	0.045		CH*NH*	0.031
(±)-G**1**/**1 b**	CHO*H*	0.025	(±)-G**6**/**1 a**	O*CH*$_3$	0.005
	*CH*OH	0.016		*CH*OH	0.024
	*CH*NH	0.022	(±)-G**6**/**1 b**	O*CH*$_3$	0.007
(±)-G**1**/**1 c**	O*CH*$_3$	0.011	(±)-G**7**/**1 a**	*CH*$_2$CHNH	0.012
	*CH*OH	0.020		O*CH*$_3$	0.005
	*CH*NH	0.010		O*CH*$_3$	0.015
(±)-G**2**/**1 a**	*CH*$_3$	0.003		*CH*OH	0.043
	O*CH*$_3$	0.028	(±)-G**7**/**1 b**	*CH*$_2$CHNH	0.015
	*CH*OH	0.067			0.006
	CO*NH*	0.073	(±)-G**7**/**1 c**	*CH*$_2$CHNH	0.011
(±)-G**2**/**1 b**	CHO*H*	0.040			0.006
	O*CH*$_3$	0.003	(±)-G**8**/**1 a**	O*CH*$_3$	0.022
	*CH*NH	0.007		*CH*OH	0.064
	*CH*OH	0.011		CO*NH*	0.055
(±)-G**2**/**1 c**	*CH*$_3$	0.004	(±)-G**8**/**1 b**	CO*NH*	0.031
	O*CH*$_3$	0.012	(±)-G**8**/**1 c**	O*CH*$_3$	0.010
	*CH*NH	0.007		*CH*OH	0.019
	*CH*OH	0.020		CO*NH*	0.029
(±)-G**3**/**1 a**	CHO*H*	0.069	(±)-G**9**/**1 a**	Ph*CH*$_2$	0.005
	O*CH*$_3$	0.031		CHO*H*	0.054
	*CH*NH	0.020		O*CH*$_3$	0.029
	*CH*OH	0.078		*CH*OH	0.074
	CO*NH*	0.053		CO*NH*	0.054
(±)-G**3**/**1 b**	*CH*NH	0.008	(±)-G**9**/**1 b**	*CH*OH	0.008
	*CH*OH	0.012	(±)-G**9**/**1 c**	O*CH*$_3$	0.010
(±)-G**3**/**1 c**	CHO*H*	0.032		*CH*OH	0.021
	O*CH*$_3$	0.015		CO*NH*	0.028
	*CH*NH	0.007	(±)-G**10**/**1 a**	CHO*H*	0.050
	*CH*OH	0.030		O*CH*$_3$	0.028
	CO*NH*	0.026		*CH*OH	0.065
(±)-G**4**/**1 a**	O*CH*$_3$	0.039	(±)-G**10**/**1 b**	*CH*$_2$CH	0.005
	*CH*OH	0.079	(±)-G**10**/**1 c**	O*CH*$_3$	0.010
	CO*NH*	0.071	(±)-G**11**/**1 a**	O*CH*$_3$	0.032
(±)-G**4**/**1 b**	O*CH*$_3$	0.006		*CH*OH	0.078
	*CH*OH	0.015	(±)-G**11**/**1 b**	CHO*H*	0.047
	CO*NH*	0.062		O*CH*$_3$	0.005
(±)-G**4**/**1 c**	CHO*H*	0.047	(±)-G**11**/**1 c**	O*CH*$_3$	0.013
	O*CH*$_3$	0.020		*CH*OH	0.019
	*CH*OH	0.025	(±)-G**12**/**1 a**	O*CH*$_3$	0.017
(±)-G**5**/**1 a**	O*CH*$_3$	0.026		*CH*OH	0.061
	*CH*OH	0.072		CO*NH*	0.065
	CO*NH*	0.053	(±)-G**12**/**1 b**	*CH*OH	0.018
(±)-G**5**/**1 b**	CHO*H*	0.027	(±)-G**12**/**1 c**	CHO*H*	0.030
	*CH*OH	0.013		*CH*OH	0.008
	CO*NH*	0.032			

[a] TAMCSA **1 a**/**1 b**/**1 c** : (±)-G**X** = 1 : 1 (molar ratio), **X** = **1**–**12**, [(±)-G**X**] = 10 mM.

As shown in table 2, in most cases, enantiomers of (±)-G**1**–**12** were clearly differentiated by the split ^{1}H NMR signals of multiple types of protons with the assistance of TAMCSAs **1 a**–**1 c**. Furthermore, when compared with their ^{1}H NMR spectra of the same guests in the presence of TAMCSAs **1 b** and **1 c**, TAMCSA **1 a** proved to be superior, since not only their ΔΔδ values are larger, but also at least one well-resolved ^{1}H NMR signal of the split protons is exhibited. These results indicate that TAMCSA **1 a** is a highly effective and sensitive chiral solvating agent towards these chiral ester derivatives by ^{1}H NMR spectroscopy. Partial ^{1}H NMR spectra of the most representative proton (*CH*OH) of (±)-G**1**–**12** in the presence of TAMCSA **1 a** are shown in Table 3.

In order to compare the chiral discriminating capability of TAMCSAs **1 a**–**1 c** as a function of the macrocyclic structural features, compound **2 a** was used as chiral solvating agent for exploring discrimination of enantiomers of (±)-G**1**–**3** at a concentration of 10 mM and 1 : 1 molar ratio of host and guest in $CDCl_3$. However, the split ^{1}H NMR signals of any protons of enantiomers of (±)-G**1**–**3** were not observed in the ^{1}H NMR spectra. The results indicate that the 12-membered macrocyclic

Table 3. Partial ^{1}H NMR spectra of the *CH* protons (*CH*OH group) of (±)-G**1**–**12** in the presence of TAMCSA **1 a** in $CDCl_3$ (400 MHz).[a]

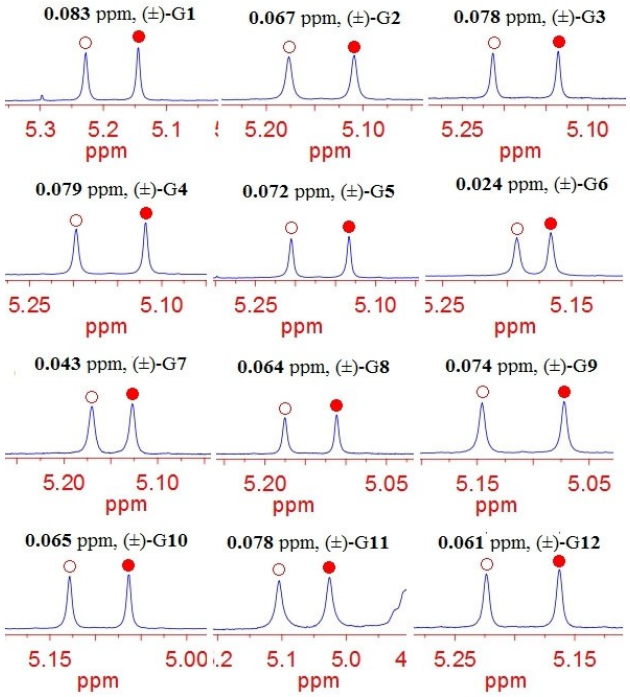

[a] TAMCSA **1 a** : (±)-G**X** = 1 : 1 (molar ratio), **X** = **1**–**12**, [TAMCSA **1 a**] = 10 mM.

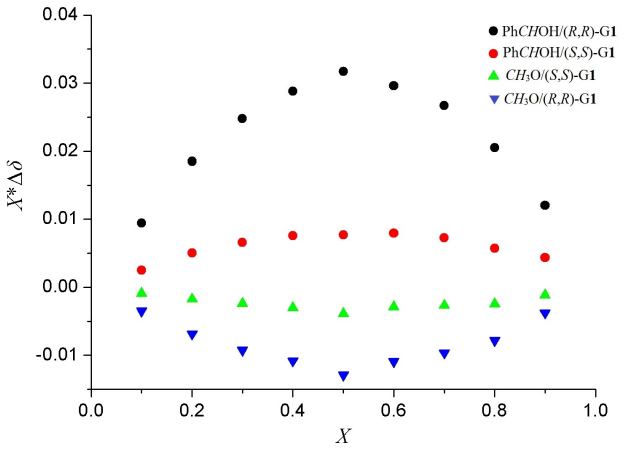

Figure 3. Job plots for complexes of (*S*,*S*)-G**1** and (*R*,*R*)-G**1** with TAMCSA **1 a**. Δδ stands for chemical shift change of Ph*CH*OH of (*R*,*R*)-G**1** (●) and (*S*,*S*)-G**1** (●), and CH_3O of (*R*,*R*)-G**1** (▲) and (*S*,*S*)-G**1** (▼) in the presence of TAMCSA **1 a** in $CDCl_3$ (400 MHz). *X* stands for the molar fraction of (±)-G**1**, *X* = [(±)-G**1**]/[(±)-G**1** + TAMCSA **1 a**].

structure of TAMCSAs **1 a**–**1 c** is a key and decisive factor towards chiral discrimination of these chiral ester derivatives.

In order to better understand the chiral discriminating behavior of (±)-G**1**–**12** induced by TAMCSAs **1 a**–**1 c**, samples of (±)-G**1** with TAMCSA **1 a** (molar fraction ranging from 0.1 to 0.9) were prepared with a total concentration of 10 mM in $CDCl_3$, and their ^{1}H NMR spectra were measured on a 400 MHz spectrometer. Job plots of (*S*,*S*)-G**1** and (*R*,*R*)-G**1** were obtained in the presence of TAMCSA **1 a** by recording the change of chemical shifts of two types of protons (Ph*CH*OH and CH_3O groups) of (*S*,*S*)-G**1** and (*R*,*R*)-G**1** in the context of the continuous variation Job's method.[18] The results showed that the maximum values 0.024 ppm (Ph*CH*OH, $X^*\Delta\delta = X^*\Delta\delta_{(R,R)} - X^*\Delta\delta_{(S,S)} = 0.031–0.007$), and 0.009 ppm ($CH_3$O, $X^*\Delta\delta = X^*\Delta\delta_{(S,S)} - X^*\Delta\delta_{(R,R)} = -0.0039–(-0.0129)$) were reached at a molar fraction of $X = 0.5$, suggesting that a pair of diastereoisomeric complexes with 1 : 1 stoichiometry are formed between (*S*,*S*)-G**1** and (*R*,*R*)-G**1** with TAMCSA **1 a**, respectively (Figure 3).

To explore the hydrogen bonding interactions between enantiomers of (±)-G**1**–**12** with TAMCSAs **1 a**–**1 c**, ^{1}H NMR titration of (*S*,*S*)-G**1** and (*R*,*R*)-G**1** were carried out in the presence of TAMCSA **1 a**, as a representative example, and their association constants (K_a) were calculated by the nonlinear curve fitting method (see SI, Table S1).[19]

To further understand the intermolecular interactions between enantiomers of (±)-G**1**–**12** with TAMCSAs **1 a**–**1 c**, theoretical calculation of (*R*,*R*)-G**1** and (*S*,*S*)-G**1** with TAMCSA **1 a** was performed by the hybrid density functional theory (B3LYP/3-21G).[20] The proposed models show that intermolecular hydrogen bonds were found between (*R*,*R*)-G**1** with TAMCSA **1 a** (CONH···OH (guest), 1.775 Å and NHCO···HO (guest), 1.632 Å (Figure 4(a)) and (*S*,*S*)-G**1** with TAMCSA **1 a** (CONH···OH (guest), 1.793 Å and NHCO···HO (guest), 1.625 Å) (Figure 4(b)), respectively.

Meanwhile, the calculated chemical shift values (δ, ppm) and nonequivalent chemical shifts (Δδ, ppm) of the *CH* proton (Ph*CH*OH group) of (*R*,*R*)-G**1** and (*S*,*S*)-G**1** in the presence of TAMCSA **1 a** were obtained based on the aforementioned theoretically calculated models and shown to be in agreement with the observed δ values in $CDCl_3$ (see SI, Table S2).

Now that the chiral discriminating capability of TAMCSAs **1 a**–**1 c** has been demonstrated towards chiral ester derivatives containing an amide group and possessing one or two stereogenic centers by means of ^{1}H NMR spectroscopy, their practical application was evaluated in analyzing and determining enantiomeric excess (ee). Therefore, samples containing (*R*,*R*)-G**1** with 0 %, 5 %, 10 %, 30 %, 50 %, 70 %, 90 %, 95 % and 98 % ee were prepared in the presence of TAMCSA **1 a** in $CDCl_3$, and their ^{1}H NMR spectra were measured on a 400 MHz spectrometer. The separated ^{1}H NMR signals of the *CH* proton (Ph*CH*OH group) of (*R*,*R*)-G**1** and (*S*,*S*)-G**1** were used for analysis and determination of enantiomeric excesses, since they were clearly observed in their ^{1}H NMR spectra without any signal overlap or other interference. The ee values of all samples with different optical purities were calculated by the integration of ^{1}H NMR signals of the *CH* proton of (*R*,*R*)-G**1** and (*S*,*S*)-G**1** (up to 98 % ee) (Figure 5(a)). Excellent linear correlations between the theoretical (*X*) and observed (*Y*) ee values are obtained in the presence of TAMCSA **1 a** (Figure 5(b)).

In order to further evaluate practical applications in the determination of enantiomeric excess, another set of samples of G**9** containing (*R*,*R*)-G**9** with 0 %, 10 %, 30 %, 50 %, 70 %, 90 % and 95 % ee was prepared in the presence of TAMCSA **1 a**

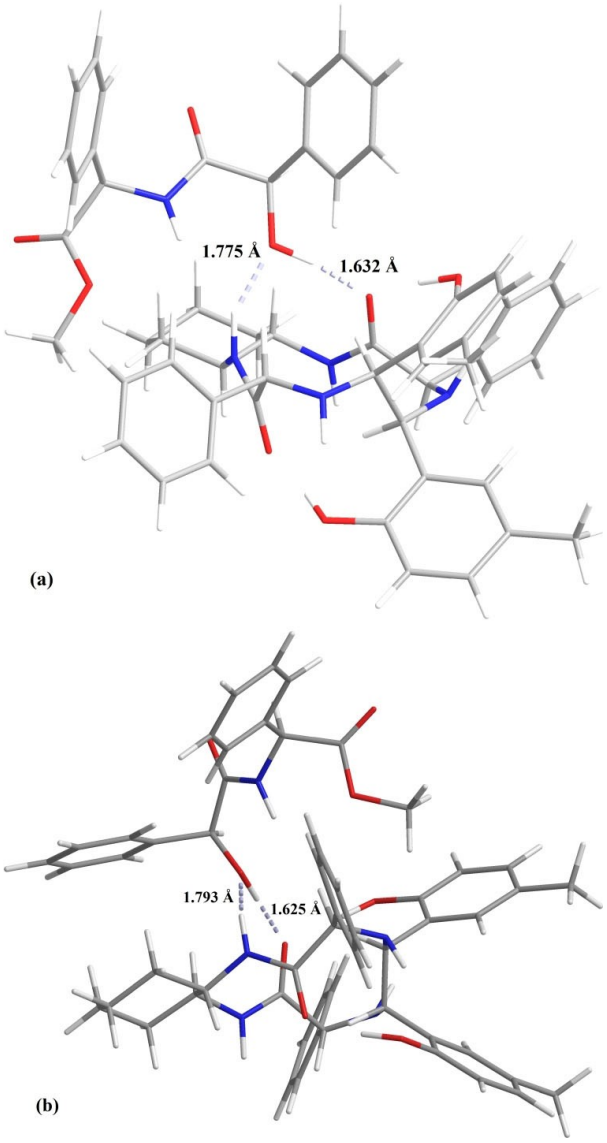

Figure 4. Proposed DFT models for the hydrogen bonding interactions between (*R*,*R*)-G**1** (a) and (*S*,*S*)-G**1** (b) with TAMCSA **1 a**, respectively.

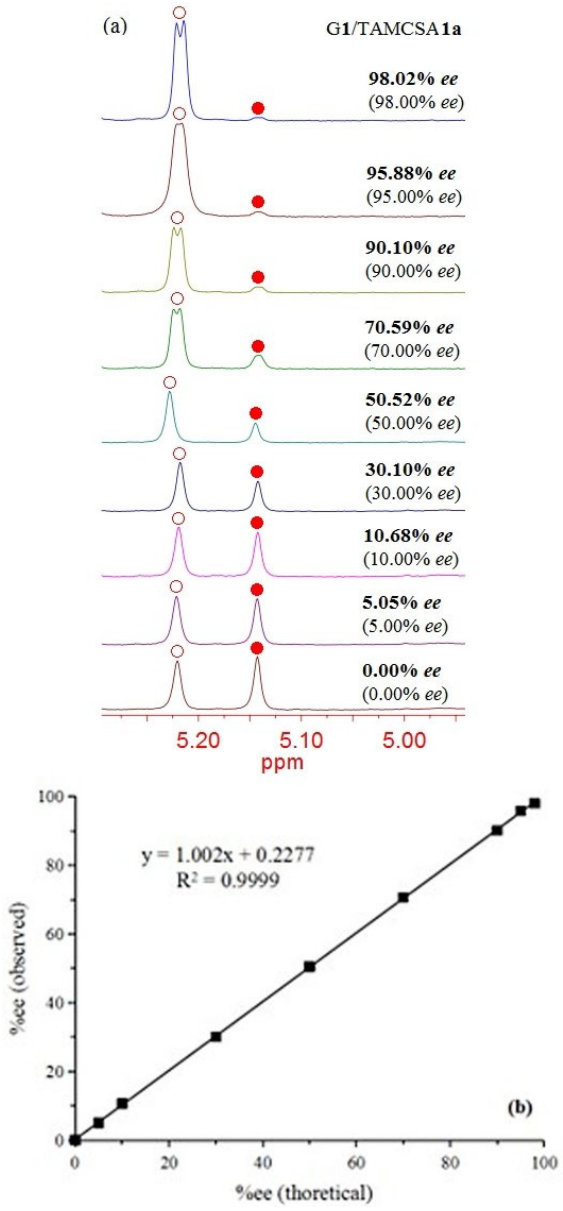

Figure 5. Determination of enantiomeric excesses (ee) of G**1** with different optical purities, ee (%) = {[(*R*,*R*)-G**1**–(*S*,*S*)-G**1**]/[(*R*,*R*)-G**1** + (*S*,*S*)-G**1**]} × 100 %. Overlaid ^{1}H NMR spectra of the *CH* proton (Ph*CH*OH) of G**1** in the presence of an equal amount of TAMCSA **1 a** (a). Linear correlation between the theoretical (*X*) and observed (*Y*) values of G**1** with TAMCSA **1 a** (b).

under the same conditions, and their ^{1}H NMR spectra were recorded on a 400 MHz spectrometer. Similarly, enantiomeric excesses of all samples were calculated by the integration of ^{1}H NMR signals of the *CH* proton of Ph*CH*OH group of (*R*,*R*)-G**9** and (*S*,*S*)-G**9** (up to 95 % ee) (see SI, Figure S3(a)). Excellent linear correlation between the theoretical (*X*) and observed (*Y*) ee values are once again obtained in the presence of TAMCSA **1 a** (see SI, Figure S3(b)).

Conclusion

Enantiomers of a new class of chiral ester derivatives containing an amide group and possessing one or two stereogenic centers (±)-G**1**–**12** have been synthesized by the amidation reaction of (*R*)- or (*S*)-mandelic acid with (*R*)- or (*S*)-α-amino acid methyl esters, and methyl 2-aminoacetate. The enantiomers of these ester derivatives, as a new class of chiral substrates, were successfully differentiated in the presence of TAMCSAs **1 a**–**1 c** by means of ^{1}H NMR spectroscopy. By analyzing and comparing chiral discriminating results, we found that TAMCSA **1 a** is a more effective and sensitive chiral solvating agent than **1 b** and **1 c** towards these ester derivatives. In order to investigate chiral discriminating behavior of chiral ester derivatives in the presence of TAMCSAs **1 a**–**1 c**, Job plots of (*R*,*R*)-G**1** and (*S*,*S*)-G**1** were performed in the presence of TAMCSA **1 a**. The results suggest that (*S*,*S*)-G**1** and (*R*,*R*)-G**1** with TAMCSA **1 a** formed a pair of diastereoisomeric complexes with 1 : 1 stoichiometry.

Meanwhile, in order to further understand hydrogen bonding interactions, the association constants (K_a) and theoretical calculation of (*S*,*S*)-G**1** and (*R*,*R*)-G**1** with TAMCSA **1a** were performed, respectively. To evaluate the practical application in analyzing optical purities of chiral substrates, enantiomeric excesses of G**1** and G**9** with various optical purities were obtained (up to 98% ee) in the presence of TAMCSA **1a**, respectively. In summary, a practical method for discrimination of enantiomers of chiral ester derivatives containing an amide moiety, and possessing one or two stereogenic centers, has been effectively established with the assistance of TAMCSAs **1a**–**1c** by using ^{1}H NMR spectroscopy.

Experimental Section

General synthetic procedure of TAMCSAs 1a–1c: The chiral diimines **5a**–**5c** were prepared from chiral diamines **4a**–**4c** with 3,5-dibromosalicylaldehyde under reflux for 3 hours in CH_3OH in 40–94% yields. To a solution of chiral diimines **5a**–**5c** (1 mmol) in dried DMF (60 mL) were added the activated zinc powder (0.65 g, 10 mmol) and MsOH (0.96 g, 10 mmol) in dried DMF (20 mL). The mixture was stirred for 23 h under a nitrogen atmosphere from −18 to 0 °C. The reaction mixture was basified to pH = 10 with a saturated $NaHCO_3$ solution. The precipitate formed was filtered off and washed with $CHCl_3$. The organic layer was separated, and water layer was extracted with $CHCl_3$ (15 mL × 3). The combined organic phase was dried over anhydrous Na_2SO_4. The solvent was removed under reduced pressure, and the residue was purified by column chromatography on silica gel to afford TAMCSAs **1a**–**1c** in 14–20% yields and chiral compounds **2a**–**2c** as co-products in 15–20% yields.

General synthetic procedure of enantiomers of chiral ester derivatives G1–12: (*R*)- or (*S*)-mandelic acid (0.76 g, 5 mmol) was added to a suspension of *D*- or *L*-amino acid methyl ester hydrochloride (5 mmol), and methyl 2-aminoacetate hydrochloride in dried CH_2Cl_2 (8 mL) at room temperature. HOBt (5.5 mmol) and DIPEA (5.5 mmol) were added to the suspension, respectively. A solution of DCC (5.5 mmol) in dried CH_2Cl_2 (8 mL) was dropwise added to the aforementioned reaction mixture at 0 °C. After the mixture was stirred for 8 h, the precipitate was filtered off and washed with CH_2Cl_2. The solvent was removed under reduced pressure. The residue was purified by column chromatography on silica gel to afford the corresponding enantiomeric products of chiral ester derivatives G**1**–**12** in 52–74% yields.

Supporting Information Summary

The characterization data of all new chiral compounds, including ^{1}H NMR, ^{13}C NMR, HRMS and their spectra, NOESY spectra of TAMCSAs **1a**–**1c**, overlaid ^{1}H NMR of chiral discriminating condition optimizations and determination of enantiomeric excesses of G**9**, related data of density functional theory (DFT) computations, and ^{1}H NMR spectra of chiral recognition of (±)-G**1**–**12**, are provided in the Supporting Information.

Acknowledgements

This work was supported by the Scientific Research Fund Performance Award of Beijing Normal University (Award Number 10200/111203277). Work in the Missouri Lab (P. S.) was supported by the National Institute of General Medical Science of the National Institutes of Health under Award Number R15GM117508 and R15GM139071.

Conflict of Interest

The authors declare no conflict of interest.

Data Availability Statement

The data that support the findings of this study are openly available in Wiley Online Library at https://doi.org/[doi], reference number 50.

Keywords: Asymmetric synthesis · chiral ester derivatives · chiral recognition · chiral solvating agents · NMR spectroscopy

[1] a) M. L. Li, Y. Li, J. B. Pan, Y. H. Li, S. Song, S. F. Zhu, Q. L. Zhou, *ACS Catal.* **2020**, *10*, 10032–10039; b) W. W. Xu, M. Cheng, S. Y. Zhang, Q. F. Wu, Z. Liu, M. K. Dhinakaran, F. Liang, E. G. Kovaleva, H. B. Li, *Chem. Commun.* **2021**, *57*, 7480–7492; c) F. Zaera, *Chem. Soc. Rev.* **2017**, *46*, 7374–7398; d) Y. Q. Meng, J. B. Fan, M. H. Wang, W. B. Gong, J. P. Zhang, J. P. Ma, H. Y. Mi, Y. Huang, S. Yang, R. S. Ruoff, J. X. Geng, *Angew. Chem. Int. Ed.* **2022**, *61*, e202117815.

[2] a) J. M. Padró, S. Keunchkarian, *Microchem. J.* **2018**, *140*, 142–157; b) A. Calcaterra, I. D'Acquarica, *J. Pharm. Biomed. Anal.* **2018**, *147*, 323–340; c) V. K. Vashistha, A. Kumar, *Chirality* **2020**, *32*, 722–735; d) S. Thoonen, C. Hua, *Chem. Asian J.* **2021**, *16*, 890–901.

[3] a) Z. Wang, W. Q. Xiong, Z. F. Huang, G. Z. Qin, M. Zi, L. M. Yuan, *Chirality* **2022**, *34*, 462–472; b) C. Betzenbichler, L. Huber, S. Kräh, M.-L. K. Morkos, A. F. Siegle, O. Trapp, *Chirality* **2022**, *34*, 732–759.

[4] a) W. H. Pirkle, T. C. Pochapsky, *Chem. Rev.* **1989**, *89*, 347–362; b) Y. Okamoto, T. Ikai, *Chem. Soc. Rev.* **2008**, *37*, 2593–2608; c) G. Shi, Y. Li, X. Dai, J. Shen, X. H. Wan, *Chirality* **2022**, *34*, 574–586.

[5] a) S. L. Pilicer, C. Wolf, *J. Org. Chem.* **2020**, *85*, 11560–11565; b) Z. A. De los Santos, C. C. Lynch, C. Wolf, *Angew. Chem. Int. Ed.* **2019**, *58*, 1198–1202; *Angew. Chem.* **2019**, *131*, 1211–1215; c) L. L. Wang, M. Quan, T. L. Yang, Z. Chen, W. Jiang, *Angew. Chem. Int. Ed.* **2020**, *59*, 23817–23824; *Angew. Chem.* **2020**, *132*, 24025–24032.

[6] a) T. Taniguchi, K. Monde, K. Nakanishi, N. Berova, *Org. Biomol. Chem.* **2008**, *6*, 4399–4405; b) M. R. Poopari, Z. Dezhahang, K. Shen, L. Wang, T. L. Lowary, Y. J. Xu, *J. Org. Chem.* **2015**, *80*, 428–437; c) G. Pescitelli, *Chirality* **2022**, *34*, 333–363.

[7] a) X. M. Lu, J. Tang, X. X. Dang, X. L. Jing, K. L. Xu, H. Li, B. Liang, *RSC Adv.* **2017**, *7*, 13552–13560; b) L. Pu, *Angew. Chem. Int. Ed.* **2020**, *59*, 21814–21818; *Angew. Chem.* **2020**, *132*, 21998–22012.

[8] a) J. M. Seco, E. Quiñoá, R. Riguera, *Chem. Rev.* **2004**, *104*, 17–117; b) C. Aroulanda, P. Lesot, *Chirality* **2022**, *34*, 182–244.

[9] a) J. Shen, Y. Okamoto, *Chem. Rev.* **2016**, *116*, 1094–1138; b) C. J. Welch, H. William, *Chirality* **2020**, *32*, 961–974; c) C. Payne, S. R. Kass, *ChemistrySelect* **2020**, *5*, 1810–1817.

[10] a) Z. Y. Sun, F. Zhang, X. Y. Zhang, D. M. Tian, H. B. Li, *Chem. Commun.* **2015**, *51*, 4823–4826; b) S. E. Gunal, S. T. Tuncel, I. Dogan, *Tetrahedron* **2020**, *76*, 131141–131146; c) M. Quan, X. Y. Pang, W. Jiang, *Angew. Chem. Int. Ed.* **2022**, *61*, e202201258; d) X. Y. Shi, G. P. Zhang, W. Liu, Y. Jin, B. X. Li, *Chem. Commun.* **2022**, *58*, 427–430.

[11] a) D. Parker, *Chem. Rev.* **1991**, *91*, 1441–1457; b) T. J. Wenzel, J. D. Wilcox, *Chirality* **2003**, *15*, 256–270; c) S. Jang, H. Kim, *Asian J. Org. Chem.* **2021**, *10*, 886–890; d) X. B. Zhang, J. Xu, Z. F. Sun, G. L. Bian, L. Song, *RSC Adv.* **2022**, *12*, 4692–4296.

[12] a) G. W. Li, X. J. Wang, D. D. Cui, Y. F. Zhang, R. Y. Xu, S. H. Shi, L. T. Liu, M. C. Wang, H. M. Liu, X. X. Lei, *RSC Adv.* **2020**, *10*, 34605–34611; b) A. Recchimurzo, C. Micheletti, G. Uccello-Barretta, F. Balzano, *J. Org. Chem.* **2021**, *86*, 7381–7389; c) L. Z. Liu, C. G. Ma, Q. He, Y. Huang, W. G. Duan, *Org. Chem. Front.* **2021**, *8*, 4144–4152

[13] G. P. Gao, C. X. Lv, Q. J. Li, L. Ai, J. X. Zhang, *Tetrahedron Lett.* **2015**, *56*, 6742–6746.
[14] a) M. Curini, F. Epifano, F. Maltese, M. C. Marcotullio, *Tetrahedron Lett.* **2002**, *43*, 3821–3823; b) R. Dahiya, *Pak. J. Pharm. Sci.* **2007**, *20*, 317–323; c) J. Y. Li, X. Li, P. X. Zhou, L. Zhang, S. Z. Luo, J. P. Cheng, *Eur. J. Org. Chem.* **2009**, *2009*, 4486–4493.
[15] a) N. Kise, H. Oike, E. Okazaki, M. Yoshimoto, T. Shono, *J. Org. Chem.* **1995**, *60*, 3980–3992; b) N. Kise, T. Iwasaki, Y. Yasuda, T. Sakurai, *Tetrahedron Lett.* **2008**, *49*, 7074–7077.
[16] L. Feng, G. P. Gao, H. M. Zhao, L. Zheng, Y. Wang, P. Stavropoulos, L. Ai, J. X. Zhang, *J. Org. Chem.* **2018**, *83*, 13874–13887.
[17] a) N. Florini, G. F. Arnaud, B. Kónya, C. Zucchi, G. Pályi, *Tetrahedron: Asymmetry* **2009**, *20*, 1036–1039; b) S. M. Rele, S. S. Iyer, E. L. Chaikof, *Tetrahedron Lett.* **2007**, *48*, 5055–5060.
[18] a) G. Uccello-Barretta, F. Balzano, A. M. Caporusso, A. Iodice, P. Salvadori, *J. Org. Chem.* **1995**, *60*, 2227–2231; b) F. Ulatowski, K. Dąbrowa, T. Bałakier, J. Jurczak, *J. Org. Chem.* **2016**, *81*, 1746–1756.
[19] L. Fielding, *Tetrahedron* **2000**, *56*, 6151–6170.
[20] M. J. Frisch, G. W. Trucks, H. B. Schlegel, G. E. Scuseria, M. A. Robb, J. R. Cheeseman, G. Scalmani, V. Barone, B. Mennucci, G. A. Petersson, *Gaussian 16, Revision A. 03*, Gaussian, Inc., Wallingford, CT **2016**.

Submitted: October 17, 2022
Accepted: January 23, 2023